

Covering-radius and Collinearity- Minimizing Pilots for Channel Estimation in TDD Systems

Xu Zhu, Yi Zeng, and Tiejun Li

Abstract—This letter studies pilot design for orthogonal frequency-division multiplexing-based time-division duplex (TDD) systems under a sliding-window latest-slot recovery framework that jointly exploits delay–Doppler sparsity across recent slots. Under contiguous-subband and fairness constraints, this viewpoint naturally leads to a geometry-aware time–frequency joint pilot assignment. We show that effective patterns should balance grid coverage and redundant-collinearity suppression, with an additional symmetry-avoidance refinement when complete collinearity elimination is infeasible. Based on these principles, we formulate a mixed-integer construction method compatible with practical TDD allocation. Numerical results show that minimum-coverage-radius and collinearity-control (MCC) pattern improves both surrogate geometry metrics and latest-slot recovery performance.

Index Terms—Pilot pattern design, TDD systems, compressed sensing, channel estimation, time–frequency allocation

I. INTRODUCTION

SPARSE recovery or compressed sensing have been widely applied to channel estimation, and the associated pilot-design problem has also been extensively studied in the literature [1], [2]. In orthogonal frequency-division multiplexing (OFDM) systems, when each user is allocated a pilot set that is not overly limited, accurate channel recovery can often be achieved from single-slot observations alone, provided that the in-slot pilot positions are properly designed at the subcarrier level [3]–[5]. As a result, much of the existing pilot-design methodology is developed from a slot-wise viewpoint, emphasizing in-slot sensing quality and user fairness.

In practical time-division duplex (TDD) systems, however, pilot allocation is often constrained jointly by protocol and physical-layer requirements. Pilots are typically transmitted in contiguous frequency-domain blocks, and when many users are simultaneously served, each user may only occupy a relatively narrow pilot subband. As a result, recovering the full-band channel from the current slot alone becomes a large-bandwidth frequency-extrapolation problem. In slowly varying scenarios, it may therefore be preferable to carry historical channel information forward across time, while using the current-slot pilots mainly to refine the occupied subband.

A natural question is then whether better reconstruction performance can be achieved by jointly exploiting the two-

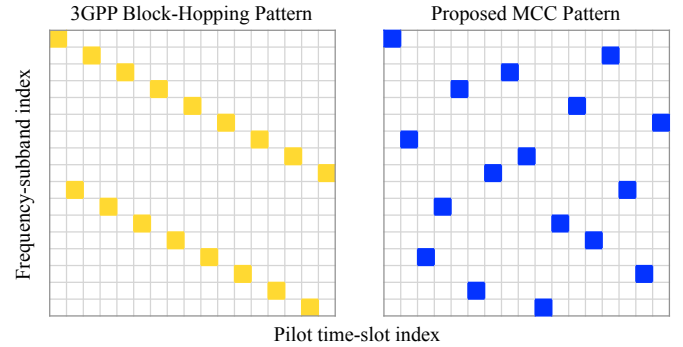


Fig. 1. Illustration of pilot base patterns on the $k \times k$ time–frequency grid ($k = 17$). Each colored square indicates an active subband–time pair (f, t) with $X_{ft} = 1$. Left: conventional 3GPP SRS-based block-hopping pattern, whose pilot blocks follow a regular linear trajectory across slots. Right: proposed MCC pattern, which spreads the pilot blocks more evenly and avoids overly repetitive collinear structures.

dimensional sparsity in the delay–Doppler (DD) domain. This observation has appeared in related delay–Doppler frameworks, especially orthogonal time frequency space (OTFS), where joint DD-domain processing is more explicit [6], [7]. However, the gain brought by DD-domain joint sparse recovery does not itself require a new modulation format. In this letter, we keep the underlying OFDM system unchanged and adopt a sliding-window latest-slot recovery viewpoint. Specifically, for a window of length T , the pilot observations from the most recent T slots are jointly used to reconstruct the DD-domain sparse channel, which is then mapped to the full-band channel of the latest slot.

Once the recovery target is changed in this way, pilot design must also be reconsidered. The relevant object is no longer an isolated in-slot pilot arrangement, but a time–frequency pattern over the whole observation window. Consequently, a regular pilot-block hopping rule that is convenient under conventional protocol design, including the 3GPP SRS-based frequency-hopping configuration specified in TS 38.211 [8] (Clause 6.4.1.4.3), can become unfavorable when judged by the multi-slot sensing criterion induced by joint recovery. Guided by the channel-extrapolation geometry and mutual-coherence considerations, we propose the MCC pilot, emphasizing *minimum coverage* radius together with *collinearity* control. The resulting design principles admit a tractable mixed-integer linear programming formulation under contiguous-subband and fairness constraints for constructing pilot patterns.

X. Zhu, Yi Zeng, and T. Li are with Laboratory of Mathematics and Applied Mathematics, School of Mathematical Sciences, Center for Machine Learning Research, Peking University, Beijing 100871, P.R. China

Email: xuzhu@pku.edu.cn (X. Zhu), zengyi0427@pku.edu.cn (Y. Zeng), tieli@pku.edu.cn (T. Li)

Corresponding author: Tiejun Li

II. SYSTEM MODEL AND DESIGN OBJECTIVE

A. TDD Pilot Allocation Pattern

We consider a simplified time–frequency resource model. At each time instant, the base station uses N subcarriers and assigns a contiguous subband of length M to each active user. Let $k = N/M$ be an integer, so that at most k users can be simultaneously supported. Define the subbands $\mathcal{B}_f := \{(f-1)M+1, \dots, fM\}$, ($f = 1, \dots, k$). At each time slot, the collection $\{\mathcal{B}_f\}_{f=1}^k$ is assigned to the k users without overlap.

To encode the pilot arrangement, we introduce a binary matrix $X \in \{0, 1\}^{k \times k}$, where the column index corresponds to time and the row index corresponds to the subband index. The feasibility conditions are

$$\sum_{f=1}^k X_{ft} = 1, \quad \forall t; \quad \sum_{t=1}^k X_{ft} = 1, \quad \forall f. \quad (1)$$

Thus, each time slot activates exactly one subband in the base pattern, and each subband is visited exactly once over one period. For user fairness, we adopt a protocol-inspired cyclic strategy: a single base pattern is designed, and different users use cyclic column shifts of that pattern. This ensures that all users share the same geometry up to a deterministic shift. Fig. 1 illustrates two representative base patterns on the $k \times k$ grid (with $k = 17$ in Fig. 1); in the figure, each colored square represents an active location (f, t) with $X_{ft} = 1$.

B. Windowed Joint-Recovery Model

Pilot design in this letter is driven by the following recovery task. For a latest slot t_0 and a short observation window $\Omega_{t_0} := \{t_0 - T + 1, \dots, t_0\}$, we jointly use the pilot observations within Ω_{t_0} to reconstruct the latest-slot full-band channel of user u . A compact observation model is

$$Y_t^{(u)} = P_t^{(u)} \Phi_t^{(u)} H_t^{(u)} + W_t^{(u)}, \quad t \in \Omega_{t_0}, \quad (2)$$

where $P_t^{(u)}$ encodes the subband selected by the pilot pattern, $\Phi_t^{(u)}$ denotes the pilot waveform or modulation operator, $H_t^{(u)}$ is the channel response at slot t , and $W_t^{(u)}$ is noise.

When the channel evolution over Ω_{t_0} is moderate, one may use a DD-domain sparse representation of the form $H_t^{(u)} \approx F \tilde{H}^{(u)} G_t^\top$, where F is the frequency–delay partial Fourier matrix, G is the time–Doppler partial Fourier matrix, and G_t denotes the row associated with slot t . This leads to the standard sparse regularized fitting problem

$$\tilde{H}_{\text{est}}^{(u)} = \arg \min_{\tilde{H}} \sum_{t \in \Omega_{t_0}} \left\| Y_t^{(u)} - P_t^{(u)} \Phi_t^{(u)} F \tilde{H} G_t^\top \right\|_2^2 + \lambda \|\tilde{H}\|_1, \quad (3)$$

and the newest-slot full-band channel is then recovered as $H_{\text{est}, t_0}^{(u)} = F \tilde{H}_{\text{est}}^{(u)} G_{t_0}^\top$. In practice, the window size T is usually modest, so (3) remains computationally realistic by the essential joint sparse structure. Equation (3) serves as the representative joint-recovery task used to evaluate different pilot patterns and can be enhanced by leveraging more sophisticated priors [9].

C. Why Multi-Slot Recovery Changes Pilot Design

Given the windowed recovery task in (3), pilot design differs from the conventional slot-wise setting in two main aspects.

First, the pilot pattern now lives on a two-dimensional time–frequency grid, so purely slot-wise optimality is no longer sufficient. A commonly used 3GPP-style block-wise hopping rule is illustrated in the left panel of Fig. 1 for odd k . To see why such a structure can become problematic under joint recovery, consider the virtual-domain correlation induced by the full-window pilot pattern. Let f_t denote the active pilot-block index at time t . For a uniformly hopped pattern as in the left panel of Fig. 1, these block locations satisfy $f_{t+1} - f_t \equiv d \pmod{k}$ for some fixed hop increment d . Although this rule is regular and implementation-friendly in each slot, its joint sensing geometry over multiple slots can be highly unfavorable. In particular, the normalized DD-domain correlation kernel satisfies

$$|K(\tau, \nu)| = \frac{1}{Mk} \left| \frac{\sin(k\pi(\nu - dM\tau))}{\sin(\pi(\nu - dM\tau))} \right| \cdot \left| \frac{\sin(M\pi\tau)}{\sin(\pi\tau)} \right|, \quad (4)$$

where the normalization is by the main peak value at $(\tau, \nu) = (0, 0)$. Hence large correlation values concentrate near the ridge $\nu - dM\tau \equiv 0 \pmod{1}$. Moreover, the strongest off-origin ambiguity occurs at $(\tau, \nu) \equiv \pm(1/(Mk), d/k) \pmod{1}$, where (4) evaluates to $\sin(\pi/k)/(M \sin(\pi/(Mk)))$, which approaches 1 as M and k grow. Therefore, a legacy pattern that is benign from a per-slot viewpoint may become highly coherent under joint multi-slot recovery. As a contrast, chirp-type pilot [10] trajectories such as $f_t \equiv t^2 \pmod{k}$ use a deliberately non-regular quadratic arrangement across slots, which reshapes the induced interference pattern and can reduce the maximum grid-point coherence close to the Welch benchmark [11]. This comparison shows that, once multiple slots are fused, pilot design is no longer a purely slot-wise hopping problem, but a genuinely two-dimensional sensing-geometry problem.

Second, practical recovery does not always use the full observation window, but may instead adopt short temporal sub-windows of different sizes. When the channel evolves slowly, a shorter window is often sufficient and reduces computational cost. On the other hand, an excessively long window may violate the local channel-consistency assumption underlying joint recovery. Therefore, in practical channel tracking, the receiver may adapt the recovery window according to operating conditions, and pilot design should not focus solely on global full-window diversity, but should also avoid locally unfavorable configurations that may severely degrade recovery under certain window choices. Motivated by this, rather than directly optimizing all possible dynamic recovery objectives, we seek a feasible matrix X satisfying (1) whose time–frequency geometry is favorable for reliable latest-slot full-band recovery and remains robust under varying sub-window sizes. To this end, we introduce two local geometric rules for time–frequency pilot allocation.

III. GEOMETRY-GUIDED DESIGN PRINCIPLES

The key message of this section is that the desired pilot pattern can be described through two main principles together

with a refinement for the practically constrained regime: 1) the pilots should cover the time–frequency grid as evenly as possible; 2) the pattern should avoid excessive repetition of the same difference vectors. When the second requirement cannot be enforced completely under the practical TDD constraints, we further refine it by suppressing symmetric collinear configurations along the same modular line.

A. Coverage-Aware Principle

We first introduce a coverage metric for the pilot pattern. For any feasible pattern X and any metric matrix $C \in \mathbb{R}_+^{k^2 \times k^2}$ on the time–frequency grid, define the distance from grid point (f, t) to its nearest pilot by

$$a_{ft}(X; C) := \min_{f', t'} \{C_{ft \rightarrow f't'} : X_{f't'} = 1\}. \quad (5)$$

A pattern with small $a_{ft}(X; C)$ provides nearby pilot support for the recovery of location (f, t) . This is especially relevant when only a shorter sub-window is used, because long extrapolation in frequency or time generally leads to larger sensitivity.

A natural worst-case quantity is the covering radius $r(X; C) := \max_{f,t} a_{ft}(X; C)$. For fixed (k, C) , let r_k denote the minimum achievable covering radius over all feasible X . We then select pilot patterns by minimizing the average distance while enforcing the optimal worst-case radius:

$$\min_X \sum_{f,t} a_{ft}(X; C) \quad \text{s.t.} \quad (1) \ \& \ a_{ft}(X; C) \leq r_k. \quad (6)$$

This criterion favors patterns that are uniformly spread across the grid without sacrificing the worst-case guarantee.

The same preference for good coverage can also be interpreted from the mutual-coherence viewpoint, in the spirit of [3], [4]. For the virtual-domain dictionary without further delay oversampling, the correlation coefficient in the two-dimensional setting can be written as

$$\rho_{i,j}^2 = \frac{1}{|\mathcal{P}|} + \frac{2}{|\mathcal{P}|^2} \sum_{(df, dt) \in \mathcal{T}_{\text{rep}}} c_{df, dt} \Gamma_{df, dt}(i, j), \quad (7)$$

where $\Gamma_{df, dt}(i, j) := \cos(2\pi(df \cdot i + dt \cdot j)/k)$, $\mathcal{T} := \{(f' - f, t' - t) : (f, t), (f', t') \in \mathcal{P}, (f, t) \neq (f', t')\}$, and $\mathcal{T}_{\text{rep}} \subseteq \mathcal{T}$ contains one representative from each antipodal pair $\{(df, dt), (-df, -dt)\}$, while $c_{df, dt}$ denotes the multiplicity of the corresponding difference class. In the exact block-subband model, the same term is further weighted by the delay-direction Dirichlet factor already contained in $K(\tau, \nu)$, which only strengthens the sensitivity to small-delay interactions.

This expression shows that clustered pilots induce many short difference vectors, which in turn tend to create concentrated coherence peaks for small virtual-domain offsets (i, j) . Here, small (i, j) refers to the relative separation between paths rather than the absolute delay–Doppler location of a path. Since practical channels usually occupy only a limited support region within the full virtual grid, such local coherence concentration degrades the resolvability of nearby paths. This explains the coverage-aware design principle above from the mutual-coherence viewpoint.

B. Redundant-Collinearity Suppression and Symmetry Refinement

Coverage alone does not control all harmful sensing interactions. A pilot pattern may be well spread in the coverage sense, yet still be overly periodic or excessively regular. Such regularity can counterintuitively increase destructive coherence among virtual-domain offsets, a phenomenon that is particularly visible for moderate instances (e.g., $k \leq 20$) arising from TDD systems pilot allocation.

From (7), the underlying mechanism is intuitive: repeated difference vectors amplify the same oscillatory component and may therefore create large coherence peaks at certain virtual offsets. Moreover, in the present two-dimensional pilot-allocation problem, the effect is shaped not only by multiplicity but also by geometry. In particular, for a fixed virtual offset (i, j) , all difference vectors (df, dt) satisfying $df \cdot i + dt \cdot j \equiv 0 \pmod{k}$ contribute with $\Gamma_{df, dt}(i, j) = 1$ and thus align maximally. This indicates that harmful configurations are associated with redundant sets of difference vectors lying on the same modular line through the origin.

For practical TDD values of k , completely eliminating redundant collinearity is often infeasible. Hence, when some collinearity cannot be avoided, it is still desirable to suppress the most harmful geometric regularity along the same modular line. The relevant refinement is suggested again by (7). If several pilot points lie on the same modular line with symmetric spacing, then the induced coherence contributions tend to reinforce one another rather than cancel out. Therefore, when redundant collinearity is unavoidable, we explicitly exclude symmetric pilot triples along the same modular line.

IV. OPTIMIZATION-BASED PATTERN CONSTRUCTION

The previous section introduced the geometry-guided design principles for robust latest-slot recovery. We now translate them into an implementable surrogate optimization model on the full $k \times k$ time–frequency grid.

A. Surrogate Formulation of the Design Principles

a) *Coverage Linearization:* In Sec. III-A, we introduced the nearest-pilot distance $a_{ft}(X; C)$ and the coverage-driven problem (6). A useful feature of (6) is that it has the form of a standard k -median-type assignment problem and therefore admits the following exact linearization:

$$\min_{X, E} \sum_{f, t, f', t'} C_{ft \rightarrow f't'} E_{ft \rightarrow f't'}, \quad (8)$$

$$\text{s.t.} \quad \sum_{f', t'} E_{ft \rightarrow f't'} = 1, \quad \forall f, t, \quad (9)$$

$$E_{ft \rightarrow f't'} \leq X_{f't'}, \quad \forall f, t, f', t', \quad (10)$$

$$E_{ft \rightarrow f't'} = 0 \quad \text{if } C_{ft \rightarrow f't'} > r_k, \quad (11)$$

$$X_{ft}, E_{ft \rightarrow f't'} \in \{0, 1\} \ \& \ \text{satisfies (1)}. \quad (12)$$

Here, the binary variable $E_{ft \rightarrow f't'}$ indicates whether grid point (f, t) is assigned to pilot location (f', t') . The restriction (11) removes assignments outside the covering radius r_k , so only nearby candidate links need to be retained in the model.

For implementation, we use the asymmetric Manhattan-type metric $C_{f_t \rightarrow f't'} := |f - f'| + [t - t' \bmod k]$, which favors both frequency proximity and temporally recent pilot support. The asymmetry in time is motivated by the fact that, within a local recovery window, estimating the channel at the newest time index can only exploit pilot information from the current or earlier slots.

b) Redundant-Collinearity Budget and Symmetry Control: Section III-B shows that harmful coherence is closely related to repeated difference vectors and, more specifically, to redundant collections of differences lying on the same modular line. Directly modeling this mechanism in the difference-vector domain would lead to a much harder quadratic assignment-type formulation. We therefore introduce an observation-domain surrogate that captures the same geometric effect by limiting the number of modular lines that may contain collinear pilot triples:

$$\sum_{(f,t) \in \mathcal{I}} X_{f,t} \leq Z_l + 2, \quad Z_l \in \{0, 1\} \quad (\forall l \in \mathcal{S}); \quad \sum_{l \in \mathcal{S}} Z_l \leq L_r. \quad (13)$$

For each modular line l , when k is prime, at most two pilots are allowed unless the binary variable Z_l is activated, in which case a single collinear triple is admitted on that line. The budget $\sum_{l \in \mathcal{S}} Z_l \leq L_r$ then limits the total number of admissible redundant-collinearity events. We adopt this hard budget rather than a soft regularizer in order to avoid introducing an additional trade-off parameter. When k is composite, the definition $df \cdot i + dt \cdot j \equiv 0 \pmod{k}$ for all (i, j) is no longer applicable. We therefore restrict attention to modular lines induced by primitive directions (u, v) satisfying $\gcd(u, v, k) = 1$, namely, $\gcd(u, v, k) = 1$, namely $df \cdot u + dt \cdot v \equiv c \pmod{k}$, where $c = 0, \dots, k - 1$.

For the practical TDD sizes of interest, stronger four-point collinearities can typically still be excluded. When some collinear triples remain unavoidable, we further suppress symmetric multiplicity along the same modular line. For prime k , we impose

$$X_{ft} + X_{f-d,t(l,-d)} + X_{f+d,t(l,+d)} \leq 2, \quad (\forall l, d, f, t), \quad (14)$$

where $t(l, \pm d)$ denotes the corresponding time index on modular line l when the subband index is shifted from f to $f \pm d$. When k is composite, (14) is interpreted with respect to the primitive-direction-based modular-line representation above.

B. Integrated Mixed-Integer Linear Programming Formulation

Combining (8)–(14), we obtain the integrated mixed-integer linear programming (MILP)

$$\min_{X, E, Z} \sum_{f, t, f', t'} C_{f_t \rightarrow f't'} E_{f_t \rightarrow f't'} \quad \text{s.t. (9)–(14)}. \quad (15)$$

For the TDD regimes of interest, (15) remains a moderate-scale 0–1 mixed-integer linear programming and can therefore be solved directly by Gurobi. In implementation, the budget L_r can be selected by gradually tightening the admissible redundant-collinearity level until further tightening becomes infeasible or noticeably harms coverage.

V. NUMERICAL VALIDATION

We evaluate the sliding-window latest-slot recovery task on 3 km/h CDL-B channels generated by the Matlab 5G Toolbox. Unless otherwise stated, each plotted value is the median over 200 channel realizations. Since a feasible pilot pattern may appear with any of its k cyclic shifts in practice, robustness across shifts is also important. Therefore, for each channel realization, we evaluate all k cyclic shifts of the pattern, compute the latest-slot NMSE for each shift, select the worst $\lfloor k/4 \rfloor$ values, and average them. The plotted performance is then the median of this worst-quarter average over the 200 realizations. In this way, the reported curves reflect not only the average recovery accuracy but also robustness to unfavorable cyclic shifts.

For each fixed cyclic shift, (3) is solved by FISTA [12] with 500 iterations, together with virtual-domain refinement and Doppler-spread-based truncation. The regularization parameter is set as $\lambda = \sqrt{2\bar{\sigma}_{t_0}^2 N_\tau N_\nu \log(N_\tau N_\nu) / (MT)}$, where $\bar{\sigma}_{t_0}^2 := \frac{1}{T} \sum_{t \in \Omega_{t_0}} \sigma_t^2$, N_τ and N_ν denote the numbers of delay and Doppler grid points, respectively. We compare the proposed MCC pilot with the following baselines: 1) a regular 3GPP SRS-based block-hopping pattern in Fig. 1, given by $f_t \equiv f_0 + t \lfloor k/2 \rfloor \pmod{k}$ for odd k , and by the interleaved progression $f_t \equiv f_0 + \lfloor t/2 \rfloor + (k/2)(t \bmod 2) \pmod{k}$ for even k ; 2) the chirp pattern $f_t \equiv t^2 \pmod{k}$ introduced in Sec. II-C; 3) random feasible patterns, generated independently for each channel realization; and 4) two ablations of the proposed design, namely “coverage only” and “collinearity only.” All optimized pilot patterns are solved to zero optimality gap, except that the MCC pilot for $k = 19$ is terminated at a dual gap of 0.05.

Fig. 2 shows that coverage is the primary design factor for latest-slot recovery: the coverage-only pattern remains competitive in the SNR and sub-window sweeps, whereas the collinearity-only pattern is consistently inferior. The benefit of collinearity control becomes clearer in harder regimes, especially as the pilot transmission interval increases. The sweep over k further shows that some values, notably the composite case $k = 16$, may induce unfavorable regular structure and visible performance loss. By comparison, the chirp pattern is motivated mainly by full-window coherence and is therefore less robust over short sub-windows. Overall, the proposed MCC pilot delivers the most stable performance across the tested settings.

VI. CONCLUSION

This letter studied pilot-pattern design for sliding-window latest-slot recovery in TDD systems under practical contiguous-subband and fairness constraints. By shifting the design viewpoint from conventional slot-wise estimation to multi-slot joint recovery on the time–frequency grid, we showed that effective pilot patterns should be designed jointly across the observation window rather than slot by slot. This viewpoint leads to two main principles: coverage, which reflects the geometry of channel-extrapolation capability, and redundant-collinearity suppression, which mitigates unfavorable regular structure in more challenging regimes. Although

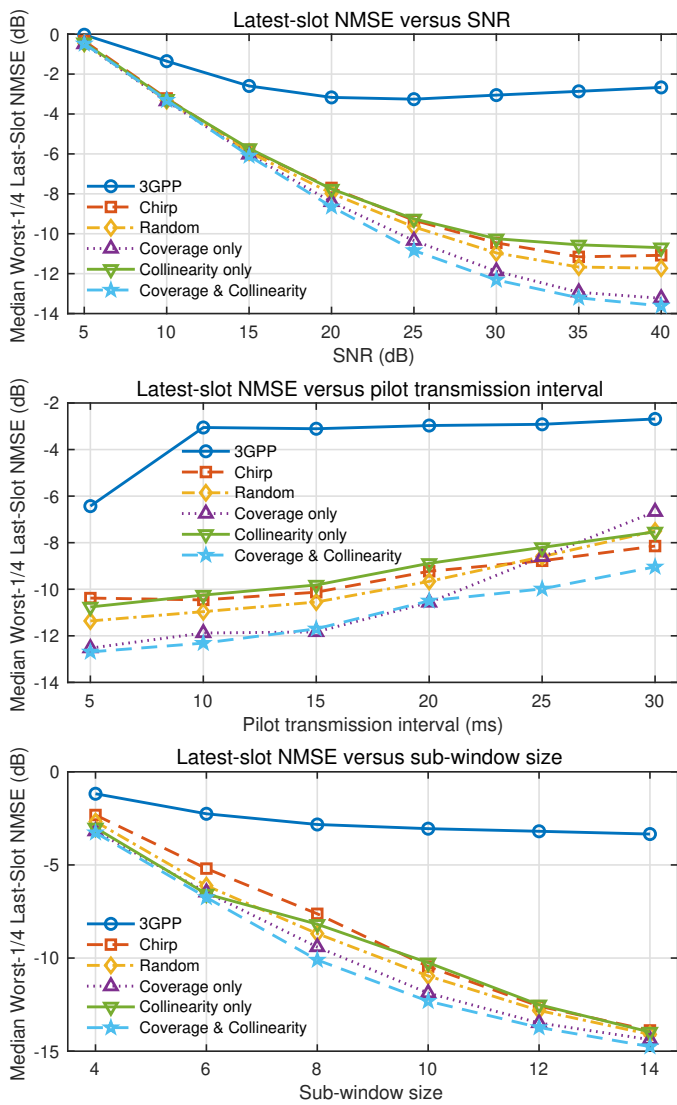


Fig. 2. Latest-slot recovery performance under sliding-window joint estimation for $k = 17$ ($M = 24$). (a) NMSE versus SNR. (b) NMSE versus pilot transmission interval. (c) NMSE versus sub-window size. The “3GPP pilot” refers to the pattern in Fig. 1. The “coverage only” design removes (13) and (14), while the “collinearity only” design minimizes only the redundant-collinearity term subject to (14). “Coverage & Collinearity” denotes the proposed MCC pilot.

these principles are realized through geometric surrogates on time–frequency point pairs that target worst-case pilot configurations, they yield designs that are computationally tractable and robust across different window sizes, pilot transmission intervals, and hopping periods.

ACKNOWLEDGMENT

The authors acknowledge the support from National Key R&D Program of China under grant 2021YFA1003301, and National Science Foundation of China under grant 12288101.

REFERENCES

[1] W. U. Bajwa, J. Haupt, A. M. Sayeed, and R. Nowak, “Compressed channel sensing: A new approach to estimating sparse multipath channels,” *Proceedings of the IEEE*, vol. 98, no. 6, pp. 1058–1076, 2010.

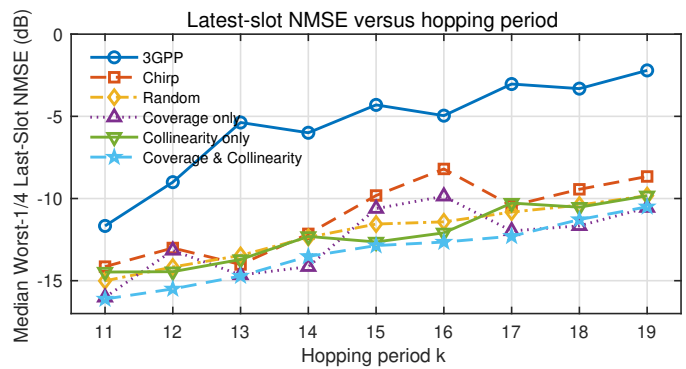


Fig. 3. Latest-slot NMSE versus hopping period k ($M = \lfloor 408/k \rfloor$), with sub-window size 10, SNR = 30 dB, and pilot transmission interval = 10 ms. The sweep includes both prime and composite values of k to illustrate the robustness of different pilot patterns to the underlying modular structure.

[2] C. R. Berger, Z. Wang, J. Huang, and S. Zhou, “Application of compressive sensing to sparse channel estimation,” *IEEE Communications Magazine*, vol. 48, no. 11, pp. 164–174, 2010.

[3] P. Pakrooh, A. Amini, and F. Marvasti, “OFDM pilot allocation for sparse channel estimation,” *EURASIP Journal on Advances in Signal Processing*, vol. 2012, no. 1, p. 59, 2012.

[4] C. Qi, G. Yue, L. Wu, Y. Huang, and A. Nallanathan, “Pilot design schemes for sparse channel estimation in OFDM systems,” *IEEE Transactions on Vehicular Technology*, vol. 64, no. 4, pp. 1493–1505, 2014.

[5] Y. Wan, A. Liu, and T. Q. Quek, “Multi-user pilot pattern optimization for channel extrapolation in 5G NR systems,” *IEEE Transactions on Wireless Communications*, 2025.

[6] R. Hadani, S. Rakib, M. Tsatsanis, A. Monk, A. J. Goldsmith, A. F. Molisch, and R. Calderbank, “Orthogonal time frequency space modulation,” in *2017 IEEE wireless communications and networking conference (WCNC)*. IEEE, 2017, pp. 1–6.

[7] P. Raviteja, K. T. Phan, and Y. Hong, “Embedded pilot-aided channel estimation for OTFS in delay–Doppler channels,” *IEEE transactions on vehicular technology*, vol. 68, no. 5, pp. 4906–4917, 2019.

[8] ETSI 3rd Generation Partnership Project (3GPP), “5G; NR; Physical channels and modulation (3GPP TS 38.211 version 18.5.0 Release 18),” ETSI, Technical Specification ETSI TS 138 211 V18.5.0, Jan. 2025, release 18.

[9] Y. Ma, X. Zhu, and T. Li, “DDA-Net: Accurate TDD channel estimation via deep unfolding the Doppler-delay-angle representation of channel signals,” 2026.

[10] L. Applebaum, S. D. Howard, S. Searle, and R. Calderbank, “Chirp sensing codes: Deterministic compressed sensing measurements for fast recovery,” *Applied and Computational Harmonic Analysis*, vol. 26, no. 2, pp. 283–290, 2009.

[11] L. Welch, “Lower bounds on the maximum cross correlation of signals (corresp.),” *IEEE Transactions on Information theory*, vol. 20, no. 3, pp. 397–399, 1974.

[12] A. Beck and M. Teboulle, “A fast iterative shrinkage-thresholding algorithm for linear inverse problems,” *SIAM Journal on Imaging Sciences*, vol. 2, no. 1, pp. 183–202, 2009.